Cell Stem Cell
Article

Cell
PRESS

Myc Represses Primitive Endoderm Differentiation in Pluripotent Stem Cells

Keriayn N. Smith,[1] Amar M. Singh,[1] and Stephen Dalton[1,*]
[1]Department of Biochemistry and Molecular Biology, Paul D. Coverdell Center for Biomedical and Health Sciences, The University of Georgia, 500 D.W. Brooks Drive, Athens, GA 30602, USA
*Correspondence: sdalton@uga.edu
DOI 10.1016/j.stem.2010.06.023

SUMMARY

The generation of induced pluripotent stem cells (iPSCs) provides a novel method to facilitate investigations into the mechanisms that control stem cell pluripotency and self-renewal. Myc has previously been shown to be critical for murine embryonic stem cell (mESC) maintenance, while also enhancing directed reprogramming of fibroblasts by effecting widespread changes in gene expression. Despite several studies identifying in vivo target genes, the precise mechanism by which Myc regulates pluripotency remains unknown. Here we report that codeletion of c- and N-MYC in iPSCs and ESCs results in their spontaneous differentiation to primitive endoderm. We show that Myc sustains pluripotency through repression of the primitive endoderm master regulator GATA6, while also contributing to cell cycle control by regulation of the *mir-17-92* miRNA cluster. Our findings demonstrate the indispensable requirement for c- or N-myc in pluripotency beyond proliferative and metabolic control.

INTRODUCTION

Myc is widely regarded as being important for stem cell proliferation, but its role in the regulation of pluripotency remains unclear. To determine the role of Myc in mESCs, a multitude of genome-wide chromatin immunoprecipitation analyses (ChIP-Chip, ChIP-Seq) have been performed (Chen et al., 2008; Kidder et al., 2008; Kim et al., 2008; Sridharan et al., 2009). Despite the identification of cell cycle control and metabolic genes as direct targets, lineage-specific regulators have not been functionally defined. These data therefore leave open the question of how Myc maintains the self-renewing, pluripotent state.

The establishment of pluripotency has been widely analyzed by reprogramming somatic cells via the introduction of four exogenous factors, Oct4, Sox2, Klf4, and c-myc (Takahashi and Yamanaka, 2006). Although the exogenous introduction of c-myc is not absolutely required for reprogramming, it significantly enhances the efficiency of iPSC generation by causing sweeping changes to gene expression (Nakagawa et al., 2008; Sridharan et al., 2009). These data indicate that c-myc is important in initializing reprogramming but do not address its role in

maintenance of the pluripotent state. Dramatic changes in the mode of cell cycle regulation accompany somatic cell reprogramming, a facet of pluripotent cell biology that is widely thought to be under the control of Myc (Singh and Dalton, 2009). However, mechanisms by which Myc controls the cell cycle in pluripotent cells remain undefined.

We previously demonstrated that c-myc promotes self-renewal of mESCs in the absence of leukemia inhibitor factor (LIF), while overexpression of a dominant-negative c-myc promotes differentiation (Cartwright et al., 2005). More recently, enforced expression of Myc has been shown to promote a meta-stable pluripotent state in mESCs that are otherwise unstable (Hanna et al., 2009). Interpretation of these data, however, is confounded by observations that c-myc and N-myc knockout mice develop well past the blastocyst stage of development and that mESCs derived from these mice self-renew in a manner comparable to wild-type cells (Baudino et al., 2002; Charron et al., 1990). This can be attributed to the functional redundancy between Myc family members and their overlapping expression during early development (Malynn et al., 2000).

In this report, we address this issue by analyzing the effects of simultaneous c- and N-MYC inactivation in pluripotent stem cells. Myc is shown to impact on self-renewal through regulation of the cell cycle regulatory network and to maintain pluripotency by imposing a primitive endoderm differentiation blockade involving the master regulator GATA6.

RESULTS

Myc Is Essential for the Maintenance of Pluripotency and Inhibits Primitive Endoderm Formation

To examine the requirement for Myc in pluripotent stem cells, we generated iPSCs from mouse embryonic fibroblasts containing c-MYC and N-MYC floxed alleles via Oct4, Sox2, and Klf4 retroviruses. Flox miPSCs (c-MYC$^{fl/fl}$;N-MYC$^{fl/fl}$) have a mESC-like domed-shaped colony morphology, express markers of pluripotency, are capable of multilineage differentiation in vitro, and form teratomas in vivo (Figure S1 available online). After transfection of CreGFP, c-MYC$^{fl/fl}$;N-MYC$^{fl/fl}$ miPSCs were subjected to FACS and genotyped to confirm deletion of c- and N-MYC (Figures 1A and 1B). Upon plating of cells into mESC medium, GFP$^+$ double knockout (dKO; c-myc$^{\Delta/\Delta}$;N-myc$^{\Delta/\Delta}$) cells underwent spontaneous differentiation, as determined by loss of alkaline phosphatase staining and by loss of a tightly packed colony morphology (Figures 1C and 1D). c-MYC$^{fl/fl}$;N-MYC$^{fl/fl}$ mESCs were used in parallel experiments and generated similar results (Figures S2A and S2B). Simultaneous loss of c- and
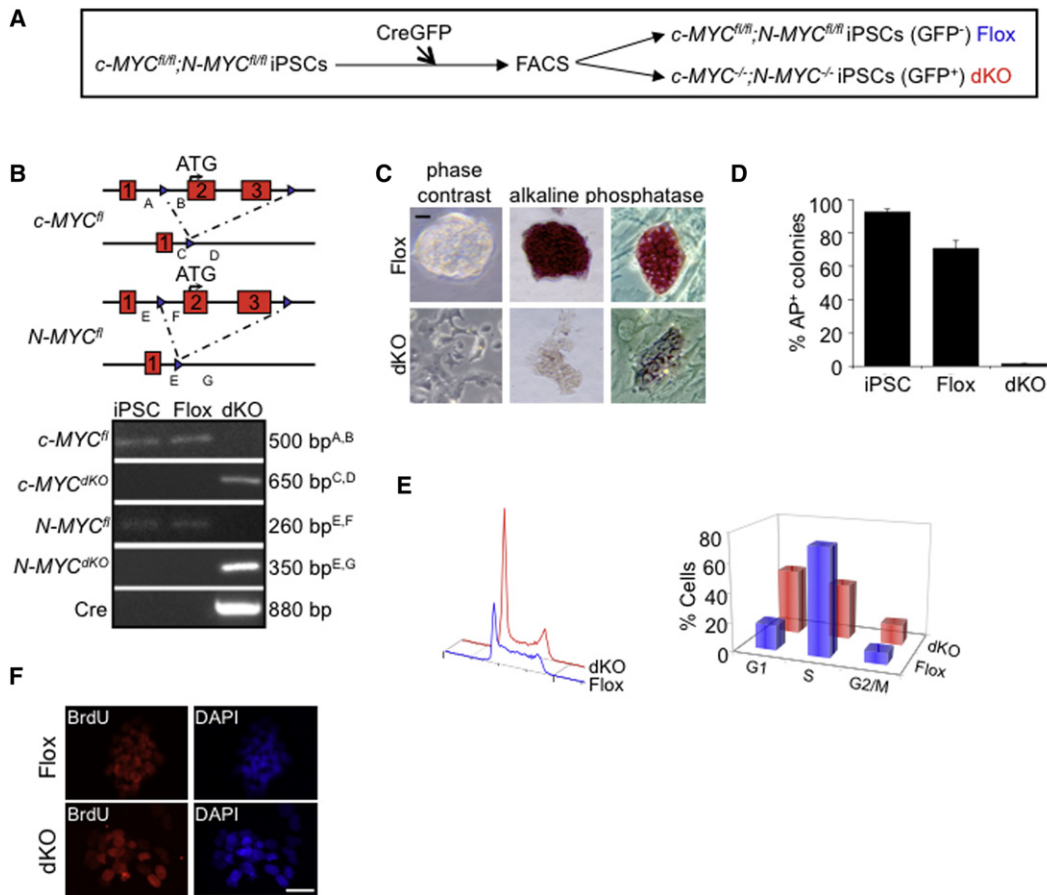
Figure 1. Deletion of c- and N-myc in iPSCs Results in Loss of Self-Renewal

(A) Derivation of double knockout c-*myc*; N-myc miPSCs by transfection of CreGFP and isolation by FACS.

(B) Locus map of targeted alleles and genotype analysis. Genotype analysis was performed on genomic DNA isolated from parental c-MYC^{fl/fl};N-MYC^{fl/fl}, CreGFP[−] (Flox) miPSCs, and CreGFP[+] (dKO) miPSCs. Amplicon lengths and corresponding primer sets corresponding to their position at the c-MYC and N-MYC loci are indicated.

(C) c-MYC^{fl/fl};N-MYC^{fl/fl} miPSCs transfected with CreGFP were FACS isolated to separate dKO and Flox cells. GFP[−] (Flox) and GFP[+] (dKO) cells were then plated in mESC medium for 3 days. Left: phase contrast images of dKO and Flox cells on gelatin. Middle and right: images of dKO and Flox cells after alkaline phosphatase staining on gelatin and mouse embryo fibroblast feeders, respectively. Scale bar represents 100 μm.

(D) Quantitative analysis of alkaline phosphatase staining for wild-type miPSCs, Flox, and dKO cells. n > 150, for each condition.

(E) Left: cell cycle profiles of propidium iodide-stained Flox and dKO cells obtained by flow cytometric analyses. Right: percent of Flox and dKO cells in G1-, S-, and G2/M-phases of the cell cycle as determined by flow cytometry analysis.

(F) Immunostaining demonstrates dKO cells remain proliferative, compared to Flox cells, by BrdU incorporation after labeling for 24 hr. Scale bar represents 100 μm.

See also Figure S1.

N-myc is therefore not compatible with maintenance of pluripotent cells.

Because Myc is widely regarded as a critical regulator of the cell cycle and cellular proliferation (Meyer and Penn, 2008), we examined the cell cycle profile and proliferative capacity of dKO cells. Not surprisingly, dKO cells showed a lengthening of G1 and G2/M and a decrease in the percentage of S-phase cells (Figure 1E). Such cell cycle remodeling is typical as mESCs undergo differentiation (Stead et al., 2002; White et al., 2005). dKO cells also had reduced uptake of BrdU relative to Flox cells after a 2 hr pulse (data not shown), but were >90% labeled after a 24 hr BrdU pulse, indicating that they remain proliferative (Figure 1F). This is consistent with the cell cycle changes seen as

pluripotent cells differentiate toward endoderm and mesoderm lineages after LIF withdrawal (Stead et al., 2002). c- and N-MYC deletion led to only small changes in apoptosis as determined by Tunel staining (data not shown).

We next set out to determine whether there was lineage-specific differentiation upon c- and N-MYC deletion. Quantitative reverse-transcriptase PCR (qRT-PCR) and immunostaining were performed on Flox and dKO cells cultured in mESC medium (Figures 2A and 2B). Significant increases in transcript levels for primitive endoderm markers were observed (Gata6 and FoxA2) but not for the early mesoderm marker Brachyury and the primitive ectoderm marker Fgf5. Similarly, mESC-derived dKO cells also displayed increases in endoderm marker
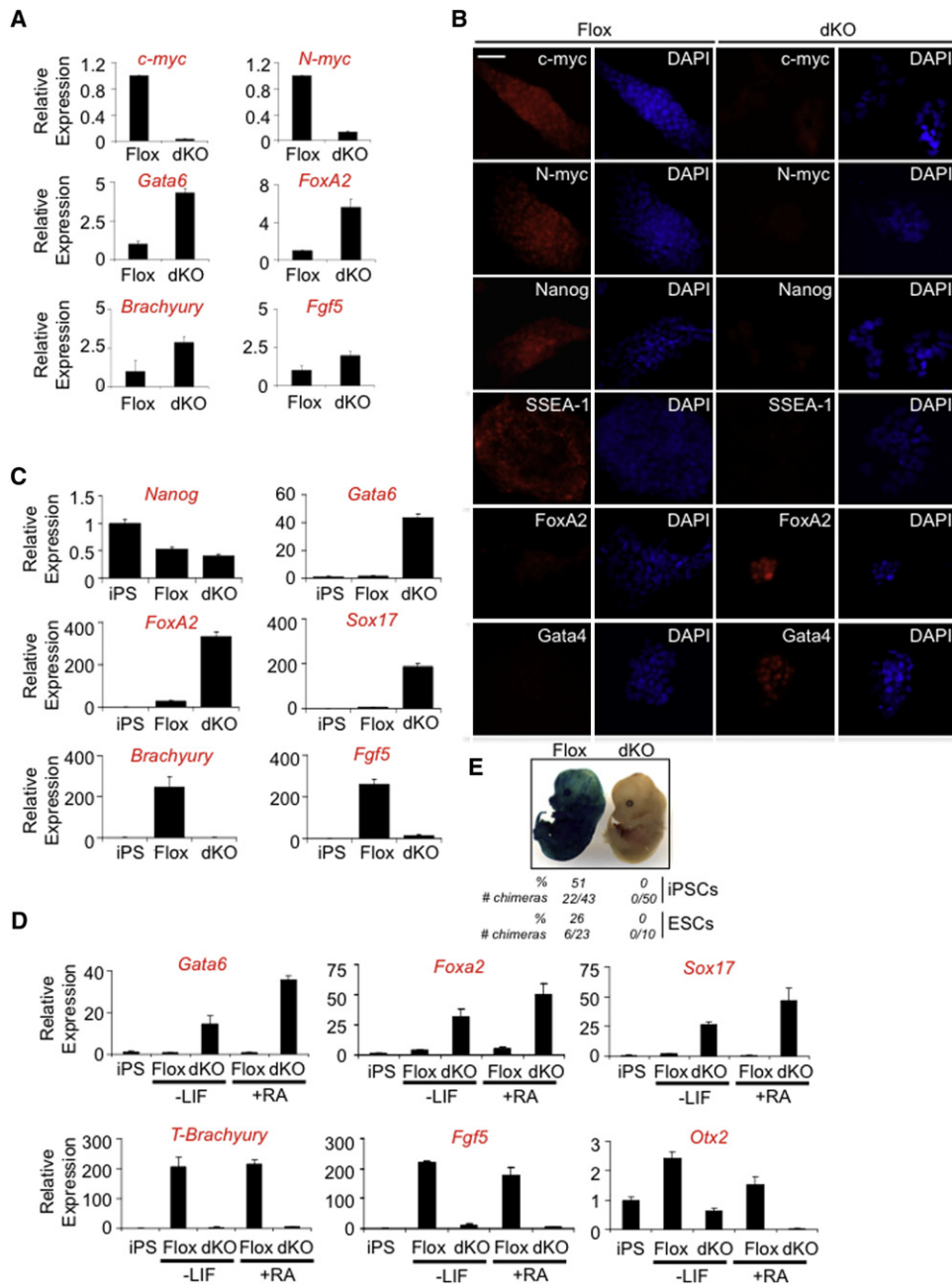
Figure 2. Deletion of c- and N-myc in iPSCs Results in Differentiation to Primitive Endoderm

(A) qRT-PCR of *c-myc*, *N-myc*, endoderm (*Gata6* and *Foxa2*), mesoderm (*Brachyury*), and primitive ectoderm (*Fgf5*) markers indicate endoderm differentiation in dKO cells compared to Flox cells. Cells were cultured in the presence of LIF and experiments were performed in triplicate, normalized to *GAPDH*, and represented as mean ± SD.

(B) Immunostaining for c-*myc*, N-myc, pluripotency markers, Nanog, and SSEA-1 and endoderm markers FoxA2 and Gata4 reveals the spontaneous differentiation to endoderm after loss of Myc in miPSCs cultured in LIF. Scale bar represents 100 μm.

(C) qRT-PCR examining *Nanog*, *Gata6*, *Foxa2*, *Sox17*, *Brachyury*, and *Fgf5* transcripts in miPSCs cultured in LIF (iPS), and during embryoid body differentiation (Flox, dKO) indicates that the loss of Myc predisposes miPSCs to primitive endoderm differentiation. Experiments were performed in triplicate, normalized to *GAPDH*, and represented as mean ± SD.

(D) qRT-PCR analysis of endoderm markers, *Gata6*, *Foxa2*, and *Sox17*; mesendoderm marker, *Brachyury*; primitive ectoderm marker, *Fgf5*; and ectoderm marker *Otx2*, 4 days after LIF removal with and without retinoic acid. iPSC represents control miPSCs cultured in the presence of LIF. Triplicate experiments were performed, normalized to *GAPDH*, and represented as mean ± SD.

(E) Flox and dKO miPSCs and mESCs expressing β-galactosidase were injected into blastocyst-stage C57BL/6 embryos, transferred into recipient females, and allowed to develop until E14.5. LacZ staining was then performed on fixed, whole embryos. The number of blastocysts injected, the number of chimeras generated, and the percent of chimeras generated are indicated.

See also Figure S2.

transcripts (Figure S2C). Immunostaining revealed that the majority of dKO cells were positive for Gata4 and FoxA2 with a decrease in expression in pluripotent stem cell markers Nanog and SSEA1. These results indicate that when cultured under normal maintenance conditions, dKO cells undergo differentiation to primitive endoderm.

To further explore the differentiation potential of dKO cells, in vitro differentiation was performed in suspension culture after FACS in the absence of LIF (Figure 2C). Additionally, differentiation was carried out in adherent culture in the absence of LIF and in the presence or absence of retinoic acid (Figure 2D). In both cases, marker transcript levels were compared to miPSCs cultured in mESC medium. Regardless of whether dKO cells were cultured in the absence of LIF only or in the presence of retinoic acid, they consistently upregulated the primitive endoderm markers *Gata6*, *FoxA2*, and *Sox17* (Figures 2C and 2D). No upregulation of the mesoderm marker *Brachyury*, primitive ectoderm marker *Fgf5*, or neuroectoderm marker *Otx2* was observed under these conditions (Figures 2C and 2D). Flox cells, however, did upregulate these other lineage markers under these conditions, indicating that dKO cells have a more restricted differentiation potential relative to Flox cells. Injection of GFP⁻ (Flox) miPSCs and mESCs into blastocysts resulted in incorporation and broad contribution to embryos, whereas GFP⁺ (dKO) cells failed to generate chimeras (Figure 2E). dKO cells therefore fail to retain pluripotency and are predisposed to become primitive endoderm.

Either c- or N-myc Is Sufficient to Maintain Pluripotency

Previously, c-MYC null mESCs were found to retain the potential for self-renewal with slight changes in differentiation capacity (Baudino et al., 2002). Because N-myc can functionally compensate for loss of c-*myc* in early embryonic development (Malynn et al., 2000), this suggested a potential overlapping role with c-*myc* in pluripotency. To evaluate the ability of different Myc family members to promote pluripotency, c-, N-, or L-mycER were introduced into dKO cells and assayed for their ability to generate alkaline phosphatase-positive colonies in the presence or absence of 4-hydroxytamoxifen (4OHT; Figure 3A). c-mycER and N-mycER, but not L-mycER, maintained the pluripotent state as determined by alkaline phosphatase staining (Figure 3B; Figure S3). Both c- and N-mycER were able to maintain dKO cells in an undifferentiated state in the presence of 4OHT for multiple passages (data not shown).

To further confirm that Myc blocks primitive endoderm differentiation, CreGFP-transfected dKO cells (GFP⁺) were plated for 3 days in mESC media ± 4OHT. qRT-PCR analysis showed that activation of N-mycER strongly suppressed the upregulation of endoderm markers *FoxA2* and *Sox17* (Figure 3C). These data demonstrate that either c- or N-myc, but not L-myc, is sufficient to maintain pluripotency and explain how single knockout c- or N-myc mESCs are able to self-renew in a comparable manner to wild-type cells (see Baudino et al., 2002; Charron et al., 1990).

Myc Targets the *mir-17-92* Cluster that Impacts on the Pluripotent Cell Cycle

Our data show that after deletion of c- and N-MYC, pluripotent cells remodel their cell cycle and differentiate into primitive endo-

derm. To understand mechanisms of Myc-mediated cell cycle regulation and endoderm repression, we set out to identify in vivo targets for c-*myc* by ChIP-Chip analysis. Previous studies (Kidder et al., 2008; Kim et al., 2008) identified in vivo Myc targets in mESCs but these did not provide any insight into our observations relating to loss of pluripotency in dKO cells. Because the potential existed that critical in vivo targets may have been missed by previous studies, we generated new tools that could expose new Myc target genes. Our approach was to generate c-*myc*^{Δ/Δ} mESC lines expressing epitope-tagged versions of c-*myc* (c-*myc*^{Δ/6x9e10} or c-*myc*^{Δ/3xHA}). Myc tagged with multiple epitopes, combined with use of monoclonal antibodies, would then allow for the identification of targets in ChIP assays. Cell lines were selected that expressed levels of epitope-tagged Myc that were at, or below, wild-type levels (Figure S4A). Many previously identified Myc target genes such as SET, EZH2, and Mybbp1a were identified by this approach (Table S1 and Figure S4B).

Similar to the situation in cancer cells (O'Donnell et al., 2005), the *mir-17-92* cluster was also bound by c-*myc* in mESCs (Figure 4A; Table S1). The *mir-17-92* cluster was next confirmed as a target by ChIP followed by qPCR (Figure 4B). Because the six miRNAs within this cluster (*mir-17*, *mir-18a*, *mir-19a*, *mir-20a*, *mir-19b-1*, and *mir-92a-1*) are coregulated through the activity of a common promoter (O'Donnell et al., 2005), responses of the *mir-17-92* cluster to changes in Myc activity were evaluated by assaying one of the transcripts, *mir-20a*. Deletion of c- and N-MYC in miPSCs resulted in a >5-fold decrease in *mir-20a* transcript levels (Figure 4C). Furthermore, when c-mycER was activated by addition of 4OHT in mESCs, there was a significant increase in *mir-20a* transcripts above existing levels (Figure 4D). These data confirm that the *mir-17-92* cluster is directly regulated by c-*myc* in pluripotent cells.

The *mir-17-92* miRNA cluster has previously been shown to control the cell cycle and facilitate cancer cell proliferation (Mendell, 2008; Yu et al., 2008) by directly blocking the expression of various cell cycle control genes such as E2F1 (O'Donnell et al., 2005), cyclin D1 (Yu et al., 2008), p21 (Fontana et al., 2008), and Rb2/p130 (Wang et al., 2008). These *mir-17-92* targets are not expressed in pluripotent cells but are upregulated during differentiation, coinciding with changes in cell cycle regulation (White et al., 2005). As anticipated, we found that upon deletion of c- and N-MYC in miPSCs, there was a significant increase in the expression of Rb2/p130 (Figure 4E). Next, the ability of *mir-17-92* cluster members to regulate the 3′ untranslated region of Rb2 was tested with a luciferase reporter assay. Transfection of miRNA precursors for either *mir-17* or *mir-20a* significantly reduced Rb2-luciferase reporter activity (Figure 4F). The magnitude of Rb2 luciferase activity suppression is comparable to that reported previously (Wang et al., 2008; see Discussion). miRNAs in the *mir-17-92* cluster therefore regulate cell cycle regulators such as Rb2 in pluripotent cells.

To obtain further evidence that Myc-regulated miRNAs in the *mir-17-92* cluster have functional relevance to the cell cycle in pluripotent cells, miPSCs were transfected with a specific oligonucleotide inhibitor targeting *mir-17*, another member of the cluster. Inhibition of *miR-17* in miPSCs decreased the percentage of S-phase cells (41% to 23%) and increased the percentage of G1 cells (16% to 24%) and G2/M (44% to 55%;
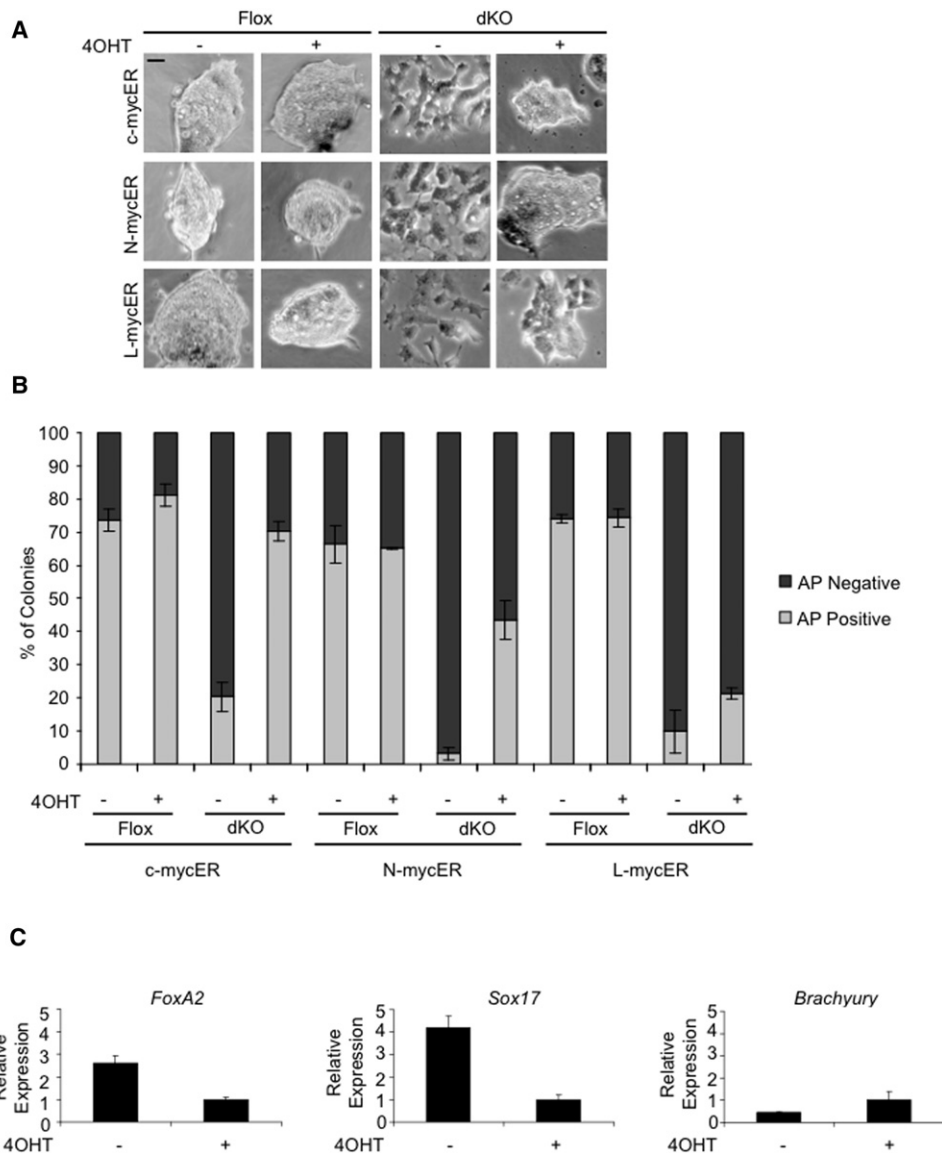
Figure 3. Conditional Activation of c- or N-myc, but Not L-myc, Is Sufficient to Maintain Pluripotency in dKO Cells

(A) Flox and dKO cell morphology after transfection with c-mycER, N-mycER, or L-mycER in the presence or absence of 4OHT for 3 days. Scale bar represents 100 μm.

(B) Quantitation of alkaline phosphatase staining (Figure S3) showing the percent positive colonies versus the percent negative colonies. n > 300 for each condition. Error bars represent mean ± SD from triplicate experiments.

(C) Activation of 4OHT-inducible N-mycER inhibits the activation of *FoxA2* and *Sox17* transcript as determined by qRT-PCR. Experiments were performed in triplicate, normalized to *GAPDH*, and represented as mean ± SD. The data are representative of multiple experiments where either c- or N-mycER-expressing cell lines were used.

See also Figure S3.

Figure 4G). Only small changes in cell cycle distribution were observed after transfection with a nontargeting siRNA control. Similar results were obtained in parallel experiments with mESCs (data not shown). Incorporation of BrdU in miPSCs was also reduced after a 24 hr pulse with introduction of antisense oligonucleotide inhibitors (Figure 4H), indicative of a cell cycle arrest or a reduction in the rate of cell division. These effects are consistent with the known ability of Myc to regulate the *miR-17-92* cluster in tumor cells (Aguda et al., 2008).

Taken together, these data indicate that Myc expression in pluripotent cells promotes the expression of the *mir-17-92* cluster, which serves to block the expression of cell cycle regulators, such as Rb2/p130. Inhibiting the activity of miRNAs within this cluster has a significant effect on cell cycle structure, most notably a dramatic reduction in the percent of S-phase cells. We therefore establish a functional link between Myc, the *miR-17-92* cluster, and cell cycle control in pluripotent cells (see Discussion).
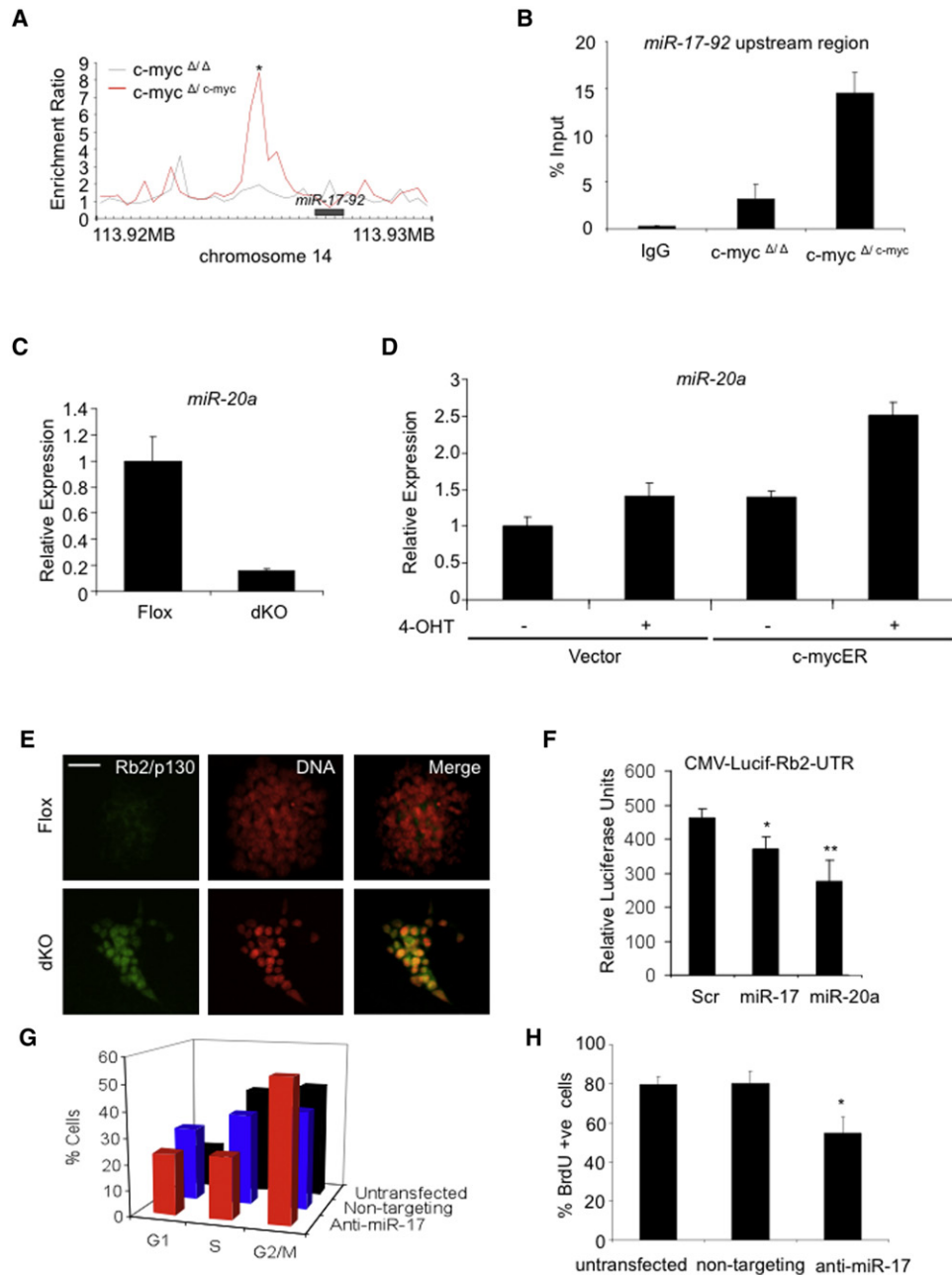
Figure 4. c-*myc* Regulates the *miR-17-92* Cluster to Control the Cell Cycle

(A) c-*myc*^{6x9e10} binds to the upstream regulatory region of the *miR-17-92* cluster in ChIP-Chip assays; *p < 0.001.

(B) Independent validation of ChIP-Chip analysis with ChIP-qPCR with the AB2.1 c-*myc*$^{\Delta/6x9e10}$ cell line. In control samples, ChIP-qPCR was carried out with chromatin immunoprecipitated by the 9e10 antibody with the c-*myc*$^{\Delta/\Delta}$ cell line and control IgG with the c-*myc*$^{\Delta/6x9e10}$ cell line.

(C) *miR-20a* transcript is downregulated upon deletion of c- and N-MYC in miPSCs.

(D) Activation of c-mycER with 4OHT in mESCs increases *miR-20a* transcript over basal levels. Experiments were performed in triplicate, normalized to *GAPDH*, and represented as mean ± SD.

(E) Increased expression of the *mir-17-92* target Rb2/p130 upon deletion of Myc in dKO cells. Flox and dKO cells were immunostained with an antibody for Rb2/p130. DNA, DAPI staining. Scale bar represents 100 μm.

(F) Myc targets *miR-17* and *miR-20a* regulate Rb2. miPSCs were transfected with a firefly luciferase reporter containing a Rb2-UTR under a CMV promoter and either a scrambled control, *miR-17* precursor, or a *miR-20a* precursor. Luciferase assays were performed in triplicate and normalized to a Renilla luciferase control. Data are representative of multiple experiments, *p < 0.05; **p < 0.01.

(G) Cell cycle profiles (flow cytometry) comparing untransfected wild-type miPSCs (black bars), cells transfected with a nontargeting control (blue bars) or cells transfected with an antisense oligonucleotide against *miR-17* (red bars). Percent of cells in G1-, S-, and G2/M-phases are shown 48 hr after transfection. Similar results were obtained in mESCs (data not shown).

Myc Inhibits Primitive Endoderm Specification by Repressing GATA6 Expression

Upon further examination of Myc-bound targets identified by ChIP-Chip in mESCs, GATA6 was also identified as a potential target (Figure 5A). As described above, *Gata6* transcript was significantly upregulated in dKO cells (Figure 2A), consistent with the possibility that Myc regulates GATA6 at the transcriptional level. Previous studies have in fact shown that GATA6 overexpression is sufficient to drive primitive endoderm differentiation of mESCs (Fujikura et al., 2002). Together, these observations suggest that Myc can inhibit primitive endoderm differentiation through regulation of GATA6. To confirm GATA6 as a Myc target, we performed scanning ChIP-qPCR analysis over the region of GATA6 corresponding to that performed in the ChIP-Chip analysis (Figure 5B). Scanning ChIP analysis confirmed that Myc binds to the GATA6 gene at several sites, including those in the 5′ upstream region and within intron 1 (corresponding to peaks 2, 5, 7, and 8).

To further evaluate the relationship between GATA6 and c-*myc* during differentiation of pluripotent stem cells to primitive endoderm, we utilized mESCs that express GFP under the control of the alpha-fetoprotein (AFP) promoter (Hamazaki et al., 2004). Upon aggregation of these cells in mESC medium (+LIF), primitive endoderm forms as the outer layer whereas the inner cells retain pluripotent properties. After aggregation for 3 days, cells were subjected to FACS followed by qRT-PCR to evaluate marker transcripts (Figure 5C). As expected, *Gata6* and *FoxA2* mRNAs were elevated in the GFP$^+$ endoderm population, whereas *Nanog* and c-*myc* transcripts were elevated in the GFP$^-$ population. These data confirm that c-*myc* is downregulated as mESCs transition to primitive endoderm. To directly confirm that GATA6 transcription is upregulated as dKO cells differentiate into primitive endoderm, nuclear run-on assays were performed. qRT-PCR analysis of RNA isolated from labeled nuclei showed that rates of GATA6 transcription increase ∼11-fold in dKO cells, relative to Flox cells (Figure 5D). Levels of FoxA2 and Sox17 nascent transcripts also increased in dKO cells, consistent with the activation of an endoderm transcriptional program after the activation of GATA6. These results indicate that Myc represses endoderm formation by blocking GATA6 transcription.

Previous studies have shown that sodium orthovanadate activates Grb2/Mek and induces Nanog downregulation and GATA6 upregulation, leading to primitive endoderm differentiation (Hamazaki et al., 2006). To determine whether c-*myc* can block the upregulation of GATA6 induced by sodium orthovanadate, c-mycER mESCs or control mESCs (vector alone) were aggregated in suspension (+LIF), in the presence or absence of sodium orthovanadate, with or without 4OHT for 24 hr (Figure 5E). qRT-PCR analysis shows that activation of c-mycER was able to block *Gata6* upregulation induced by sodium orthovanadate. *Nanog* mRNA was still downregulated when c-mycER was activated in the presence of sodium orthovanadate. These data indicate that c-*myc* is able to inhibit GATA6 expression independently of Nanog.

To investigate the effects of Myc expression on primitive endoderm formation, we activated c-mycER during embryoid body differentiation (+LIF, 3d) and examined expression of the Gata6 target, GATA4 in the primitive endoderm outer layer, which accounts for ∼3%–5% of cells in the embryoid body (Figure 5F; Hamazaki et al., 2004). Immunostaining followed by confocal microscopy revealed that activated c-*myc* (+4OHT) almost completely eliminated the expression of Gata4 in cells on the surface of embryoid bodies. We then evaluated the effects of Myc on endoderm formation in a Sox17-GFP reporter mESC line (Borowiak et al., 2009). Sox17-GFP cells were transfected with a c-*myc* expression construct or vector alone, aggregated for 48 hr in the presence of LIF, and then analyzed by flow cytometry (Figure 5G). Under these conditions, overexpression of c-*myc* reduced the number of GFP$^+$ endoderm cells by more than 50%. Altogether, these data demonstrate that c-*myc* inhibits differentiation to primitive endoderm.

To establish whether Myc prevents primitive endoderm formation by repressing GATA6, we knocked down Gata6 transcript with shRNA (Izumi et al., 2007) in dKO miPSCs. qRT-PCR analysis indicates that knockdown of Gata6 mRNA blocks the upregulation of the endoderm markers Gata4, Sox17, and Sox7 (Figure 5H). FoxA2 was not affected and so may not be directly under the control of GATA6. These data show that c-*myc* blocks primitive endoderm formation by repressing the expression of GATA6.

Even though knockdown of Gata6 in dKO cells blocks normal activation of endoderm genes, pluripotency markers such as alkaline phosphatase, Nanog, and SSEA1 are not maintained, suggesting that differentiation into other lineages may occur under these conditions (Figure S5). However, marker analysis for mesendoderm/early mesoderm, definitive endoderm, ectoderm, and trophoblast lineages after LIF withdrawal does not support this possibility (Figure 5I; Figure S5; and data not shown). Although dKO-Gata6 knockdown cells are no longer pluripotent, they fail to differentiate into any definable lineage and appear to have lost developmental potential.

DISCUSSION

We have characterized two mechanisms by which Myc contributes to self-renewal and maintenance of the pluripotent state. The first function involves maintenance of a characteristic mode of cell cycle control whereby Myc regulates the *mir-17-92* miRNA cluster. The second and perhaps most important function defined by these studies involves repression of the master endoderm regulator gene GATA6 (Morrisey et al., 1998; Koutsourakis et al., 1999).

The cell cycle profiles of pluripotent stem cells have a characteristic short G1, with a large percentage of cells in S-phase (Stead et al., 2002; Savatier et al., 1996). These cell cycle profiles are attributed to hyperphosphorylation of Rb and a lack of regulated E2F-dependent transcription. Upon differentiation, E2F and Rb family members serve to impose the restriction point near the G1/S transition leading to the remodeling of the cell

---

(H) Immunostaining monitoring the incorporation of BrdU after labeling for 24 hr demonstrates reduced cellular proliferation of cells upon transfection of antisense oligonucleotide inhibitors against *miR-17*. Assay was performed in triplicate and is represented as mean ± SD, *p < 0.05.
See also Figure S4.
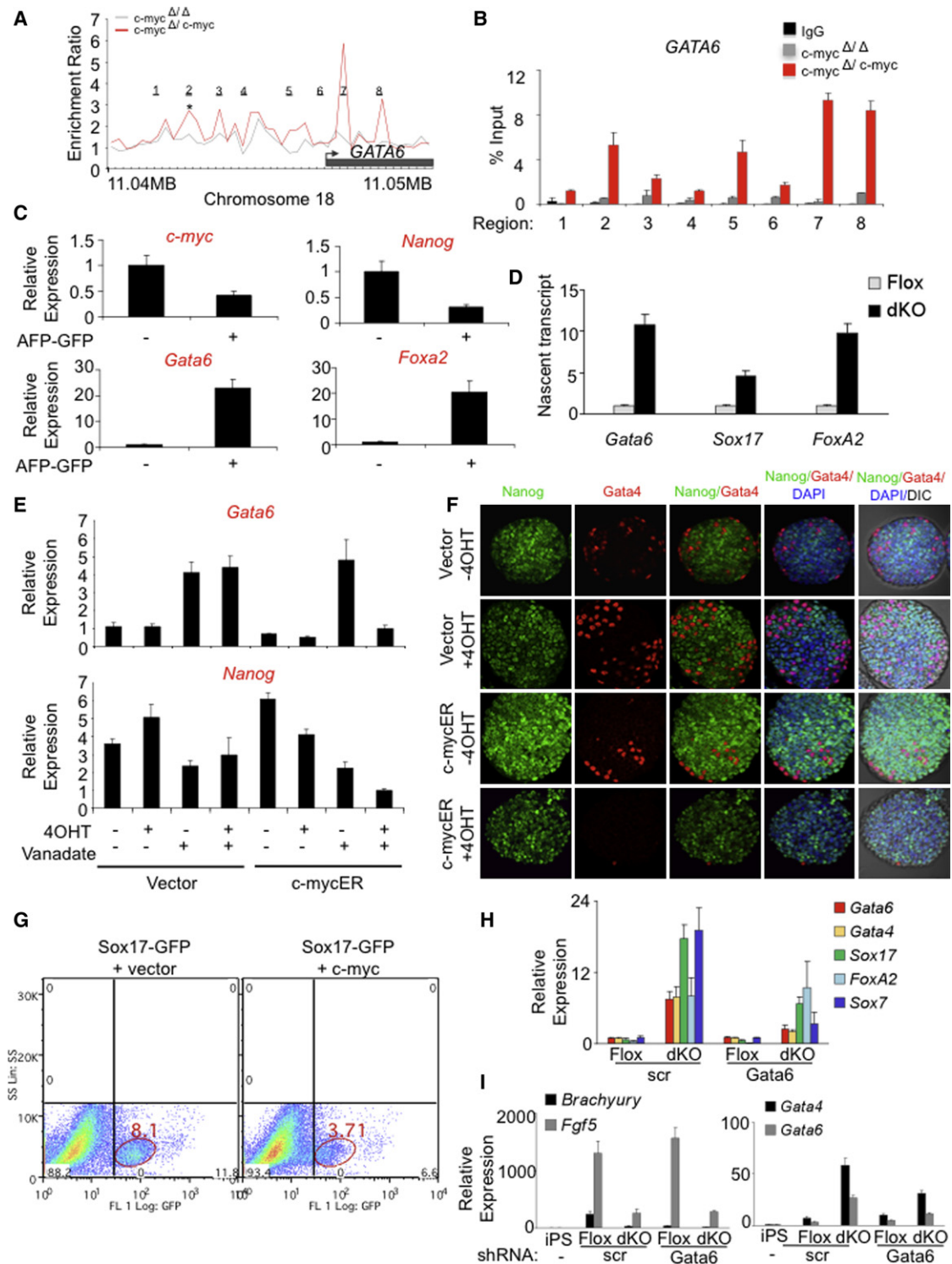
Figure 5. c-*myc* Binds and Represses the Primitive Endoderm Master Regulator GATA6 and Suppresses Primitive Endoderm Differentiation

(A) GATA6 is a Myc-bound target identified from ChIP-Chip assays; *p < 0.001.

(B) Independent validation of GATA6 as a Myc-bound target by ChIP-qPCR with eight primer sets to scan the GATA6 region corresponding to the ChIP-Chip analysis shown in (A). Primer set 2 corresponds to the statistically significant region identified by DNA Analytics software (Agilent) in the GATA6 promoter shown in (A) to bind c-*myc*. Primer sets 5, 7, and 8 also represent regions of significant enrichment and primer sets 1, 3, 4, and 6 correspond to regions not bound by c-*myc*.

(C) c-*myc* transcript is downregulated in primitive endoderm. AFP-GFP mESCs were aggregated in the presence of LIF then cultured for 3 days. GFP-positive and -negative cells were isolated by FACS and analyzed by qRT-PCR.

cycle (Savatier et al., 1996; Stead et al., 2002; White et al., 2005). The change in cell cycle structure observed upon loss of Myc—lengthening of G1 and a reduction in the percentage of S-phase cells—indicate the establishment of a checkpoint in late G1. How this dramatic switch in cell cycle regulation occurs has not been previously defined at the molecular level. However, it has been recognized for some time that changes in Myc activity could potentially orchestrate many of the cell cycle changes seen during early mESC differentiation (Cartwright et al., 2005).

The downregulation of *mir-17-92* and upregulation of cell cycle regulators, such as Rb2/p130, upon deletion of c- and N-MYC establishes one way by which Myc impacts on the cell cycle in pluripotent cells. Based on previous work, it is likely that the *mir-17-92* cluster targets other key cell cycle regulatory molecules such as E2F1, p21, and cyclin D1 (see O'Donnell et al., 2005; Cloonan et al., 2008). These are all thought to play key roles in remodeling the cell cycle as pluripotent cells transition toward differentiating lineages (Stead et al., 2002). Although *mir-17-92* has not been implicated in cell cycle control of ESCs or iPSCs previously, other miRNAs are thought to influence self-renewal, and connections between miRNAs and Myc have been established in the context of reprogramming (see Judson et al., 2009). Even though ESCs proliferate rapidly with an unusual cell cycle structure, the significance of this in relation to pluripotency remains unclear. For example, inhibition of cyclin-dependent kinases slows down the cell cycle but does not impact on pluripotency (Stead et al., 2002). Although Myc seems to be critical for maintaining rapid rates of division and the unusual cell cycle structure of pluripotent cells, it remains to be determined whether this is directly linked to the maintenance of pluripotency or to other aspects of early embryonic development, such as embryonic growth control.

Many cell cycle control genes have been previously identified as being Myc targets in pluripotent cells but our work provides a mechanistic characterization of how Myc intersects with the cell cycle machinery. Other genes identified as being Myc targets (see Kidder et al., 2008; Kim et al., 2008) are likely to be part of an orchestrated transcriptional program that establishes and maintains the pluripotent cell cycle in conjunction with the *mir-17-92* cluster. Although Myc has been proposed to regulate miRNAs in the context of cell reprogramming and

pluripotency (Judson et al., 2009), *mir-17-92* has not been previously implicated in this process. This underpins the need to understand in greater detail the relationship between Myc, miRNAs, and the establishment/maintenance of pluripotency.

During reprogramming, Myc operates during the first few days to repress fibroblast-specific genes (Sridharan et al., 2009). We speculate that during the early reprogramming stage, Myc may also serve to initiate remodeling of the cell cycle to one that is more reminiscent of a pluripotent cell. This is supported by observations that partially reprogrammed cells exhibit a cell cycle profile that is intermediate between fibroblasts and pluripotent cells (Singh and Dalton, 2009) and that cell cycle control is rate limiting for reprogramming (Edel et al., 2010). This suggests that remodeling of the cell cycle is an early event prior to, and perhaps required for, the establishment of pluripotency. The exact relationship between cell cycle regulation and establishment/maintenance of the pluripotent state still needs to be resolved. Myc is implicated in both processes, so this is an area that requires further study.

Myc Is Critical for Repression of Primitive Endoderm
In conjunction with cell cycle control, we show that Myc is required for maintenance of pluripotency by directly repressing the expression of GATA6, a master regulator of primitive endoderm formation (Morrisey et al., 1998; Koutsourakis et al., 1999). Other factors that have been implicated in Gata6 regulation, such as Nanog and Polycomb repressive complexes (Boyer et al., 2006; Singh et al., 2007), may cooperate with Myc to repress GATA6. Transcriptional control seems to be a key element of this regulation although the possibility that Myc regulates GATA6 expression at additional levels cannot be ruled out. For example, Myc-regulated miRNAs could potentially impact on Gata6 translation and mRNA stability. We are unaware, however, of any Myc-regulated miRNAs that could potentially target Gata6.

After loss of c- and N-myc, iPSCs preferentially differentiate toward primitive endoderm, even under conditions that would normally favor specification of other lineages such as after retinoic acid treatment or LIF withdrawal. Therefore, besides not being able to maintain dKO cells in a pluripotent state, they also lose the potential for differentiation into nonendoderm

---

(D) Transcription of GATA6, SOX17, and FOXA2 increases in dKO cells. Flox (GFP⁻) or dKO (GFP⁺) cells were isolated by FACS and cultured for 3 days, and nuclear run-on assays were performed by labeling nascent nuclear transcripts with biotin-16-UTP. After the isolation of biotinylated transcripts on streptavidin beads, qRT-PCR analysis was performed in triplicate. Gata6, Sox17, and FoxA2 values were normalized to GAPDH and represented as mean ± SD.

(E) Induction of *Gata6* transcript by sodium orthovanadate is blocked by activation of c-mycER. mESCs were aggregated in the presence of orthovanadate for 24 hr, in the presence or absence of 4OHT. qRT-PCR analysis was performed in triplicate and values normalized to *GAPDH* and represented as mean ± SD. Data are representative of multiple experiments.

(F) mESCs carrying a c-mycER transgene or vector alone, were aggregated for 3 days in the presence of LIF, in the presence or absence of 4OHT. Embryoid bodies were probed with antibodies for Nanog or the endoderm marker Gata4 and stained with DAPI. Embryoid bodies were analyzed by confocal microscopy and DIC optics.

(G) Sox17-GFP mESCs were transfected with vector alone or with a c-*myc* expression construct. Cells were then aggregated in the presence of LIF for 48 hr. Flow cytometry was used to determine the effect of endoderm differentiation by evaluating the percent of GFP⁺ cells.

(H) GATA6 is required for endoderm formation after loss of c- and N-Myc. c-MYC^fl/fl;N-MYC^fl/fl miPSCs were transfected with CreGFP and Gata6 shRNA or scrambled (scr) shRNA construct. GFP-positive and -negative cells were FACS sorted, plated, and analyzed after 3 days by qRT-PCR. Experiments were performed in triplicate, normalized to *GAPDH*, and represented as mean ± SD.

(I) Myc-deleted and Gata6 knockdown cells have restricted differentiation potential. c-MYC^fl/fl;N-MYC^fl/fl miPSCs were transfected with CreGFP and Gata6 shRNA or scrambled (scr) shRNA construct. Control miPSCs (iPS) were cultured in LIF, and GFP-positive (dKO) and -negative cells (Flox) were FACS sorted, aggregated in the absence of LIF to induce differentiation, and analyzed after 4 days by qRT-PCR. Experiments were performed in triplicate, normalized to *GAPDH*, and represented as mean ± SD.

See also Figure S5.

lineages. The most likely explanation for this can be accounted for by derepression of GATA6.

dKO cells also lose pluripotency after knockdown of Gata6, but fail to correctly activate the endoderm transcriptional program. These cells, however, show no signs of differentiation toward other lineages under these conditions and so appear to lack full developmental potential. This suggests that c- and N- Myc are required for differentiation of the embryonic germ layers and/or that L-myc is sufficient for endoderm differentiation. Surprisingly, Gata6 knockdown also diminished Brachyury expression. Because Gata6 is expressed in mesodermal lineages such as cardiac cells, it may play a role in regulating such mesoderm markers as Brachyury. Moreover, primitive endoderm has been implicated in patterning of embryonic germ layer derivatives, and loss of Gata6 and hence primitive endoderm cell types may impact mesoderm formation.

The identification of GATA6 as a Myc target gene was somewhat of a surprise because several other ChIP-Chip studies (Kidder et al., 2008; Kim et al., 2008) failed to detect this connection. The predisposition of dKO cells to differentiate toward primitive endoderm suggests, however, that key elements of the endoderm transcriptional program are targeted by Myc in pluripotent cells. Hence, we focused on GATA6 because of its well-known function as a primitive endoderm master regulator. It is unclear why previous studies may have overlooked the Myc-GATA6 connection but it is clear that ChIP-Chip studies are not exhaustive in their target identification, as demonstrated by differences in target genes identified by these studies (see Kidder et al., 2008; Kim et al., 2008). From a technical standpoint, Myc may weakly or transiently bind GATA6 in comparison to other loci and therefore be easily overlooked. Technically, our studies varied from other studies and used epitope-tagged Myc and corresponding monoclonal antibodies that may have allowed for the identification of target genes, such as GATA6, that would otherwise have been undetected. In addition to GATA6, our ChIP-Chip screen identified HES1 as another target of Myc in pluripotent cells. HES1, like GATA6, plays an important role in primitive endoderm development (Thomas and Beddington, 1996) and its repression by Myc may also sustain pluripotency. Further work is required to establish whether Myc also plays a role in establishing differentiation blockades on pathways other than primitive endoderm.

EXPERIMENTAL PROCEDURES

Cell Culture and Blastocyst Injections
Mouse embryonic fibroblasts isolated from c-MYC$^{fl/fl}$;N-MYC$^{fl/fl}$ embryos were used in the generation of iPSCs as described elsewhere (de Alboran et al., 2001; Knoepfler et al., 2002; Takahashi and Yamanaka, 2006). Mouse ESCs (wild-type AB2.1, AB2.1c-myc$^{\Delta/\Delta}$; Baudino et al., 2002), AFP-GFP (Hamazaki et al., 2004), Sox17-GFP (Borowiak et al., 2009), and miPSCs were cultured in LIF on gelatin-coated dishes. Differentiation was performed in adherent or suspension culture in medium without LIF. Differentiation to endoderm was performed by aggregation of cells in mESC medium, in the presence or absence of sodium orthovanadate (50 μM) and/or 4OHT (100 nM). The miRNA inhibitors, anti-miR-17 and anti-miR-20a (Ambion), miRNA precursors, pre-miR-17 and pre-miR-20a (Ambion), and nontargeting control were transfected into c-MYC$^{fl/fl}$;N-MYC$^{fl/fl}$ miPSCs and mESCs with Lipofectamine 2000 reagent (Invitrogen). Gata6 shRNA constructs were cotransfected with pCAGCreGFPiNeo via Lipofectamine2000 reagent (Invitrogen) into c-MYC$^{fl/fl}$;N-MYC$^{fl/fl}$ miPSCs. LacZ$^+$ miPSCs were generated by transfection with

a plasmid expressing the LacZ gene from the constitutive CAGi promoter, followed by selection with puromycin. Blastocyst injections and embryo analysis were performed as described previously (Cartwright et al., 2005). Mouse work was done in compliance with the University of Georgia animal use and ethics guidelines (AUP #A2008-10015).

Quantitative RT-PCR, Luciferase Assays, and Nuclear Run-on Assays
RNA was isolated with the RNeasy Mini Kit (QIAGEN), and miRNAs were isolated with the MirVana miRNA isolation kit (Ambion). qRT-PCR for mRNA and miRNA transcripts was performed by Taqman Assays (Applied Biosystems). Luciferase assays were performed with the Dual Luciferase Reporter Kit (Promega) according to instructions and analyzed on a Synergy 2 plate reader (BioTek). Nuclear run-on assays were performed by labeling RNA from isolated nuclei with biotin-16-UTP, essentially as described by Zhang et al. (2005). Biotinylated RNA was purified with streptavidin magnetic beads then reversed transcribed into cDNA. qRT-PCR transcript analysis was performed as described above.

Alkaline Phosphatase Staining, Cell Cycle Analysis, and Immunostaining
Alkaline phosphatase staining was carried out with a Leukocyte Alkaline Phosphatase staining kit (Sigma). Cell cycle analysis was performed by flow cytometry after fixing the cells in 70% ethanol and staining with propidium iodide (50 μg/ml), RNase A (200 μg/ml), and BSA (100 μg/ml) in PBS for 30 min at 37°C. Immunostaining was performed by fixing cells in 4% paraformaldehyde, blocking in 10% Donkey Serum/PBS, and incubating with the following antibodies in blocking solution: Nanog (CosmoBio); SSEA1 (Developmental Studies Hybridoma Bank); FoxA2 (Upstate); Gata4, Oct4, p130/Rb2, c-*myc* (Santa Cruz Biotechnology); N-myc (Chemicon); or BrdU (Abcam) overnight.

Chromatin Immunoprecipitation with Microarray Assays
AB2.1c-myc$^{\Delta/\Delta}$ (c-*myc* null) cell lines with stable expression of 3xHA or 6x9e10-epitope-tagged c-*myc* were used for ChIP-Chip assays (see Boyer et al., 2005). Cell lines were selected that expressed c-*myc*$^{3xHA/6x9e10}$ at levels equivalent to, or below, that of endogenous c-*myc* in the parental cell line AB2.1 to eliminate overexpression effects (Figure S4A). The negative control cell line (AB2.1c-myc$^{\Delta/\Delta}$) was generated by transfection with empty pCAGiPuro vector. Immunoprecipitations were carried out with AB2.1c-myc$^{\Delta/3xHA}$, AB2.1c-myc$^{\Delta/6x9e10}$, and AB2.1c-myc$^{\Delta/\Delta}$ cell lines via affinity-purified anti-HA, anti-9e10 monoclonal antibodies (Sigma), or control IgG. Hybridization was carried out with a Mouse Expanded Promoter ChIP-on-Chip Set (Whitehead Institute, Agilent Technologies), and validated with qPCR with SYBR Green (Bio-Rad). Targets were identified with DNA Analytics software (Agilent). Probes used to identify genomic targets were determined in a replicate whether the p value was below a predetermined cut-off (at least p < 0.05). ChIP-Chip data are expressed as an enrichment ratio of immunoprecipitated target and input DNA, calculated with DNA Analytics. Targets obtained with the AB2.1c-myc$^{\Delta/\Delta}$ cell line were subtracted from those detected with the AB2.1$^{\Delta/6x9e10}$ or AB2.1$^{\Delta/3xHA}$ cell lines and used to formulate a consensus Myc target list (Table S1). Experiments were performed in triplicate for each cell line. ChIP-qPCR data are represented as enrichment of the immunoprecipitated target relative to input DNA (Aparicio et al., 2004).

SUPPLEMENTAL INFORMATION

Supplemental Information includes five figures and one table and can be found with this article online at doi:10.1016/j.stem.2010.06.023.

ACKNOWLEDGMENTS

REFERENCES

Aguda, B.D., Kim, Y., Piper-Hunter, M.G., Friedman, A., and Marsh, C.B. (2008). MicroRNA regulation of a cancer network: Consequences of the feedback loop involving miR-17-92, E2F, and Myc. Proc. Natl. Acad. Sci. USA 105, 19678–19683.

Aparicio, O., Geisberg, J.V., Sekinger, E., Yang, A., Moqtaderi, Z., and Struhl, K. (2004). Chromatin immunoprecipitation for determining the association of proteins with specific genomic sequences in vivo. Curr. Protoc. Cell Biol. 17, 1–23.

Baudino, T.A., McKay, C., Pendevile-Samain, H., Nilsson, J.A., Maclean, K.H., White, E.L., Davis, A.C., Ihle, J.N., and Cleveland, J.L. (2002). c-Myc is essential for vasculogenesis and angiogenesis during development and tumor progression. Genes Dev. 16, 2530–2543.

Borowiak, M., Maehr, R., Chen, S., Chen, A.E., Tang, W., Fox, J.L., Schreiber, S.L., and Melton, D.A. (2009). Small molecules efficiently direct differentiation of mouse and human embryonic stem cells. Cell Stem Cell 4, 348–358.

Boyer, L.A., Lee, T.I., Cole, M.F., Johnstone, S.E., Levine, S.S., Zucker, J.P., Guenther, M.G., Kumar, R.M., Murray, H.L., Jenner, R.G., et al. (2005). Core transcriptional regulatory circuitry in human embryonic stem cells. Cell 122, 947–956.

Boyer, L.A., Plath, K., Zeitlinger, J., Brambrink, T., Medeiros, L.A., Lee, T.I., Levine, S.S., Wernig, M., Tajonar, A., Ray, M.K., et al. (2006). Polycomb complexes repress developmental regulators in murine embryonic stem cells. Nature 441, 349–353.

Cartwright, P., McLean, C., Sheppard, A., Rivett, D., Jones, K., and Dalton, S. (2005). LIF/STAT3 controls ES cell self-renewal and pluripotency by a Myc-dependent mechanism. Development 132, 885–896.

Charron, J., Malynn, B.A., Robertson, E.J., Goff, S.P., and Alt, F.W. (1990). High-frequency disruption of the N-myc gene in embryonic stem and pre-B cell lines by homologous recombination. Mol. Cell. Biol. 10, 1799–1804.

Chen, X., Xu, H., Yuan, P., Fang, F., Huss, M., Vega, V.B., Wong, E., Orlov, Y.L., Zhang, W., Jiang, J., et al. (2008). Integration of external signaling pathways with the core transcriptional network in embryonic stem cells. Cell 133, 1106–1117.

Cloonan, N., Brown, N.K., Steptoe, A.L., Wani, S., Chan, W.L., Forrest, A.R., Kolle, G., Gabrielli, B., and Grimmond, S. (2008). The mir-17-5p microRNA is a key regulator of the G1/S phase cell cycle transition. Genome Biol. 9, R127.

de Alboran, I.M., O'Hagen, R.C., Gartner, F., Malynn, B., Davidson, L., Rickert, R., Rajewsky, K., DePinho, R.A., and Alt, F.W. (2001). Analysis of C-MYC function in normal cells via conditional gene-targeted mutation. Immunity 14, 45–55.

Edel, M.J., Menchon, C., Menendez, S., Consiglio, A., Raya, A., and Izpisua Belmonte, J.C. (2010). Rem2 GTPase maintains survival of human embryonic stem cells as well as enhancing reprogramming by regulating p53 and cyclin D1. Genes Dev. 24, 561–573.

Fontana, L., Fiori, M.E., Albini, S., Cifaldi, L., Giovanni, S., Forloni, M., Boldrini, R., Donfrancesco, A., Federici, V., Giacomini, P., et al. (2008). Antagomir-17-5p abolishes the growth of therapy-resistant neuroblastoma through p21 and BIM. PLoS ONE 21, e2236.

Fujikura, J., Yamato, E., Yonemura, S., Hosoda, K., Masui, S., Nakao, K., Miyazaki, J.J., and Niwa, H. (2002). Differentiation of embryonic stem cells is induced by GATA factors. Genes Dev. 16, 784–789.

Hamazaki, T., Oka, M., Yamanaka, S., and Terada, N. (2004). Aggregation of embryonic stem cells induces Nanog repression and primitive endoderm differentiation. J. Cell Sci. 117, 5681–5686.

Hamazaki, T., Kehoe, S.M., Nakano, T., and Terada, N. (2006). The Grb2/Mek pathway represses Nanog in murine embryonic stem cells. Mol. Cell. Biol. 26, 7539–7549.

Hanna, J., Markoulaki, S., Mitalipova, M., Cheng, A.W., Cassady, J.P., Staerk, J., Carey, B.W., Lengner, C.J., Foremen, R., Love, J., et al. (2009). Metastable pluripotent states in NOD-mouse-derived ESCs. Cell Stem Cell 4, 513–524.

Izumi, N., Era, T., Akimaru, H., Yasunaga, M., and Nishikawa, S. (2007). Dissecting the molecular hierarchy for mesendoderm differentiation through a combination of embryonic stem cell culture and RNA interference. Stem Cells 25, 1664–1674.

Judson, R.L., Babiarz, J.E., Venere, M., and Blelloch, R. (2009). Embryonic stem cell-specific microRNAs promote induced pluripotency. Nat. Biotechnol. 27, 459–461.

Kidder, B., Yang, J., and Palmer, S. (2008). Stat3 and c-Myc genome-wide promoter occupancy in embryonic stem cells. PLoS ONE 3, e3932.

Kim, J., Chu, J., Shen, X., Wang, J., and Orkin, S.H. (2008). An extended transcriptional network for pluripotency of embryonic stem cells. Cell 132, 1049–1061.

Knoepfler, P.S., Cheng, P.F., and Eisenman, R.N. (2002). N-myc is essential during neurogenesis for the rapid expansion of progenitor cell populations and the inhibition of neuronal differentiation. Genes Dev. 16, 2699–2712.

Koutsourakis, M., Langeveld, A., Patient, R., Beddington, R., and Grosveld, F. (1999). The transcription factor GATA6 is essential for early extraembryonic development. Development 126, 723–732.

Malynn, B.A., de Alboran, I.M., O'Hagen, R.C., Bronson, R., Davidson, L., DePinho, R.A., and Alt, F.W. (2000). N-myc can functionally replace c-myc in murine development, cellular growth, and differentiation. Genes Dev. 14, 1390–1399.

Mendell, J.T. (2008). miRiad roles for the miR-17-92 cluster in development and disease. Cell 133, 217–222.

Meyer, N., and Penn, L.Z. (2008). Reflecting on 25 years with MYC. Nat. Rev. Cancer 8, 976–990.

Morrisey, E.E., Tang, Z., Sigrist, K., Lu, M.M., Jiang, F., Ip, H.S., and Parmacek, M.S. (1998). GATA6 regulates HNF4 and is required for differentiation of visceral endoderm in the mouse embryo. Genes Dev. 12, 3579–3590.

Nakagawa, M., Koyanagi, M., Tanabe, K., Takahashi, K., Ichisaka, T., Aoki, T., Okita, K., Mocjiduki, Y., Takizawa, N., and Yamanaka, S. (2008). Generation of induced pluripotent stem cells without Myc from mouse and human fibroblasts. Nat. Biotechnol. 26, 101–106.

O'Donnell, K.A., Wentzel, E.A., Zeller, K.I., Dang, C.V., and Mendell, J.T. (2005). c-Myc-regulated microRNAs modulate E2F1 expression. Nature 435, 839–843.

Savatier, P., Lapillonne, H., van Grunsven, L.A., Rudkin, B.B., and Samarut, J. (1996). Withdrawal of differentiation inhibitory activity/leukemia inhibitory factor up-regulates D-type cyclins and cyclin-dependent kinase inhibitors in mouse embryonic stem cells. Oncogene 12, 309–322.

Singh, A.M., and Dalton, S. (2009). The cell cycle and Myc intersect with mechanisms that regulate pluripotency and reprogramming. Cell Stem Cell 5, 141–149.

Singh, A.M., Hamazaki, T., Hankowski, K.E., and Terada, N. (2007). A heterogeneous expression pattern for Nanog in embryonic stem cells. Stem Cells 25, 2534–2542.

Sridharan, R., Tchieu, J., Mason, M.J., Yachechko, R., Kuoy, E., Horvath, S., Zhou, S., Zhou, Q., and Plath, K. (2009). Role of the murine reprogramming factors in the induction of pluripotency. Cell 136, 364–377.

Stead, E., White, J., Faast, R., Conn, S., Goldstone, S., Rathjen, J., Dhingra, U., Rathjen, P., Walker, D., and Dalton, S. (2002). Pluripotent cell division cycles are driven by ectopic Cdk2, cyclin A/E and E2F activities. Oncogene 21, 8320–8333.

Takahashi, K., and Yamanaka, S. (2006). Induction of pluripotent stem cells from mouse embryonic and adult fibroblast cultures by defined factors. Cell *126*, 663–676.

Thomas, P., and Beddington, R. (1996). Anterior primitive endoderm may be responsible for patterning the anterior neural plate in the mouse embryo. Curr. Biol. *6*, 1487–1496.

Wang, Q., Li, Y.C., Wang, J., Kong, J., Qi, Y., Quigg, R.J., and Li, X. (2008). miR-17-92 cluster accelerates adipocyte differentiation by negatively regulating tumor-suppressor Rb2/p130. Proc. Natl. Acad. Sci. USA *105*, 2889–2894.

White, J., Stead, E., Faast, R., Conn, S., Cartwright, P., and Dalton, S. (2005). Developmental activation of the Rb-E2F pathway and establishment of cell cycle-regulated cyclin-dependent kinase activity during embryonic stem cell differentiation. Mol. Biol. Cell *16*, 2018–2027.

Yu, Z., Wang, C., Wang, M., Li, Z., Casimiro, M.C., Liu, M., Wu, K., Whittle, J., Ju, X., Hyslop, T., et al. (2008). A cyclin D1/microRNA 17/20 regulatory feedback loop in control of breast cancer cell proliferation. J. Cell Biol. *182*, 509–517.

Zhang, M.-X., Ou, H., Shen, Y.H., Wang, J., Coselli, J., and Wang, X.L. (2005). Regulation of endothelial nitric oxide synthase by small RNA. Proc. Natl. Acad. Sci. USA *102*, 16967–16972.

Note Added in Proof

Further information about c- and N-Myc floxed mESCs can be found in a recently published paper (Varlakhanova, N.V., Cotterman, R.F., deVries, W.N., Morgan, J., Donhue, L.R., Murray, S., Knowles, B.B., and Knoepfler, P.S. (2010). myc maintains embryonic stem cell pluripotency and self-renewal. Differentiation *80*, 9–19.)